Available online at www.sciencedirect.com

ScienceDirect

Energy Procedia 81 (2015) 987 – 994

Energy Procedia

69th Conference of the Italian Thermal Engineering Association, ATI 2014

A study of a packed-bed thermal energy storage device: test rig, experimental and numerical results

Mario Cascetta[a]*, Giorgio Cau[a], Pierpaolo Puddu[a], Fabio Serra[b]

[a]Department of Mechanical, Chemical and Materials Engineering,University of Cagliari, Italy
[b]Solar Concentration Technologies and Hydrogen from RES Laboratory, Sardegna Ricerche, Italy

Abstract

This paper presents the experimental set-up built at the DIMCM of Cagliari University to study a thermal energy storage (TES) system based on alumina beads freely poured into a carbon steel tank using air as heat transfer fluid. The system is instrumented with several thermocouples to detect axial and radial temperature distribution as well as reservoir wall temperature. Experimental temperature distribution along the storage system was compared with the numerical ones obtained by a two-phase one dimensional Schumann model. Numerical results show good agreement with the experimental results if thermal properties are considered as temperature dependent and the experimental temperature profile at the top of the bed is used for simulations.

Peer-review under responsibility of the Scientific Committee of ATI 2014

Keywords: Packed bed, Porous media, Thermal energy storage (TES), Thermocline, Dynamical model, Experimental TES;

1. Introduction

Solar thermal plants are considered one of the most promising technologies to reduce the impact of greenhouse gases produced by conventional power plants [1]. In recent years, research activities have been devoted to improving their operation by means of thermal storage to compensate for the lack of daytime radiation for meteorological reasons or simply overnight, [2]. Thermal energy storage (TES) systems are normally useful for correcting the decoupling between the power required by users and that produced by renewable power plants. TES is present in various commercial and industrial applications, often integrated with conventional energy sources to achieve major

* Corresponding author. Tel.: +39-0706755741; fax: +39-0706755717.
E-mail address: mcascetta@unica.it

Peer-review under responsibility of the Scientific Committee of ATI 2014
doi:10.1016/j.egypro.2015.12.157

reliability by reducing peaks of electricity generation, increasing generation capacity and reducing production costs [3]. From a technological point of view, thermal storage systems can be characterized in different ways [4], but the method most widely used is based on the physical principle, so three types of thermal storage are available: sensible, latent and thermochemical [5]. In every type a sequential process of charge, storage and discharge is present.

In the first case, thermal energy is stored as sensible heat of a liquid or a solid material and represents the simplest and least expensive form of thermal storage [6]. In the second case, thermal energy is stored as latent heat [7, 8]. The third type uses an endothermic chemical reaction, where the energy associated with a reversible reaction is required for the dissociation of the chemicals [9].

The thermal storage investigated herein is of a sensible heat type and consists of a steel tank filled with alumina beads that exchange heat with a gaseous heat transfer fluid (HTF) that passes through them, thus generating a particular temperature profile, the so-called “thermocline” [10].

In past decades, the flow and heat transfer in packed beds, including random and structured packings, were extensively investigated by many researchers. The reason was the high area-to-volume ratio of the packed beds that enhances heat transfer [11]. Some correlations for particle-to-fluid forced convection heat transfer coefficient were proposed by Wakao [12] and by Gnielinski [13], while Tesfay [14] investigated the interactions between the HTF and the filler material using a dimensionless form of the Schumann model [15]. A computational study of forced convective heat transfer in structured packed beds with spherical or ellipsoidal particles was made by Yang [16].

Nomenclature

c	specific thermal capacity
d	diameter
h	heat transfer coefficient
k	thermal conductivity
L	bed height
Nu	Nusselt number
Pr	Prandtl number
Re	Reynolds number
r	tank inner radius
t	time
T	temperature
x	axial coordinate
y	radial coordinate
u	fluid velocity
V	volume

Greek symbols

α	specific surface area of the packed bed
ε	void fraction
θ	dimensionless temperature
ρ	density
μ	dynamic viscosity

Subscripts

eff	effective
f	fluid
max	maximum
min	minimum
p	particle, constant pressure
s	solid
v	constant volume

A literature review indicates that it is a common practice to employ the local thermal equilibrium (LTE) which implies that the local temperature difference between the fluid and solid phases is negligible at all locations in the system considered [17]. Accurate simulation of heat transfer in a porous medium requires a two-equation local thermal non-equilibrium approach (LTNE) with separate energy equations for simulating the fluid and the solid phases, with an additional term in each equation to take into account the energy exchanged between them.

The present work aims to attempt to contribute to the study of the thermal behavior of a porous bed. To this end, a TES system basically composed of a tank containing a packed bed of alumina beads crossed by a hot air flow, generating the so-called thermocline was built. Experimental results are compared with those generated by a one-dimensional numerical simulation, using for the Nusselt number some literature correlations.

2. Experimental setup

Figure 1a shows the simplified schematic of the test-rig built at DIMCM, where a carbon steel tank filled with small spheres of alumina is used for energy storage. The experimental set-up shown in Figure 1b allows investigation of heat transfer performance of packed beds. The heat transfer fluid that flows through the porous bed is air driven by a variable speed screw compressor before being expelled through a vent. An electric heater raises the air temperature to the desired value during the charging phase. Three 3-way stainless steel full-bore manual valves provide great flexibility in operation, and allow performance of a charging or discharging phase. Both V1 and V2 are equipped with a PTFE seat, and can be used up to 160°C, whilst a metallic seat allows V3 to work up to 350°C. Table 1 reports the most relevant data of the rig. In particular, an Atlas Copco oil-free screw compressor was used to overcome the overall pressure losses in the circuit. By changing the compressor speed with an inverter, the delivered flow rate can be varied from 255 to 940 m^3/h of free air. A customized 70 kW Watlow electrical heater can heat the air up to 300°C. The fluid temperature during the charging phase can be set by means of a PID controller, whilst during the discharging phase the minimum fluid temperature is that at the compressor output.

Table 1. Technical data of rig components.

Compressor delivered flow	255-940 m^3/h, FAD
Electrical heater max. power	70 kW
Maximum air temperature	300 °C
Bed height	1800 mm
Bed diameter	584 mm
Alumina bead diameter	7-9 mm
Alumina bead thermal conductivity (100 °C)	30 W/mK
Alumina bead density	3550 kg/m^3
Alumina bead heat capacity (100 °C)	902 J/kgK
Bed void fraction	0.385-0.395
Tank coating thickness (Mineral wool)	100 mm

The net volume of the porous bed inside the reservoir is about 0.5 m^3, 0.58 m in diameter and 1.8 m in height. The storage material is made of commercial sintered alumina beads with an average diameter of 8 mm ($Al_2O_3 \geq 89.5$ wt %), manufactured by Industrie Bitossi. The beads are freely poured into the reservoir from the top by removing a flange, whilst they can be pulled out by opening a flange nozzle at the bottom. Preliminary tests showed a bed void fraction ε of about 0.385 – 0.395. A layer of 100 mm mineral wool covers the carbon steel tank to minimize thermal losses to the outside. Two flow distributors at the top and bottom of the reservoir spread the air uniformly in the porous bed. Temperature distribution in the storage tank was carefully investigated using 19 T-type thermocouples along the vertical axis, 100 mm from each other. They were placed in a metallic rack as shown in Figure 2a. Five more thermocouples were placed by covering a radius length, with a decreasing distance from each other close to the wall to investigate the influence of the wall on thermal profile. A homemade feed-through linked the sensors to the outside. The temperature of the external wall was measured by ten K-type thermocouples along the axial direction and by five K-type thermocouples in the circumferential direction at a given height. To avoid the presence of holes in the metal wall, the sensors were applied and fastened using special high-temperature cements. The thermocouples were calibrated in the range of 25-300 °C with a precision of ± 1°C.

Other thermocouples were used to measure the flow temperature at different locations along the plant to handle the valves before starting the charging or discharging phase. A differential pressure transmitter detected the pressure drop along the bed. The mass flow rate was evaluated by a Simer orifice plate (Q in Figure 1a-1b).

All the detected signals were sent to a National Instruments Compact DAQ USB chassis with several modules for thermocouples and analog inputs. The whole plant was monitored with a Graphical User Interface developed using LabVIEW software.

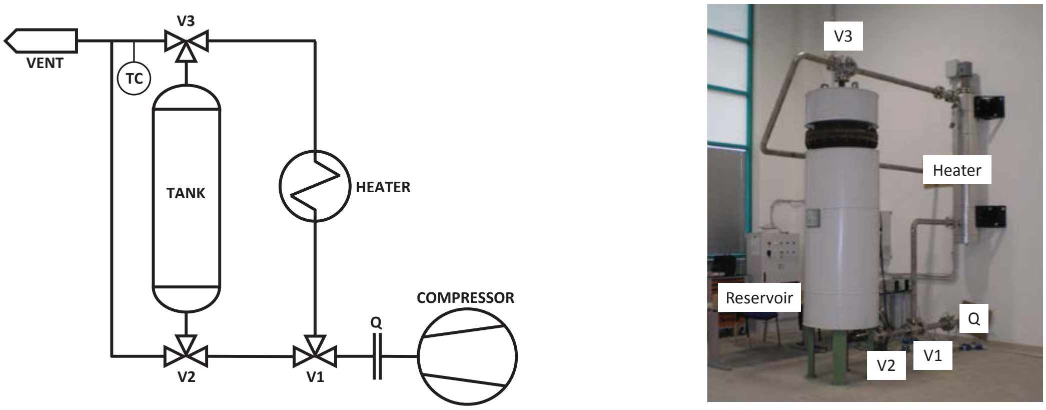

a) b)

Fig. 1. (a) schematic of laboratory test rig.; (b) laboratory test rig

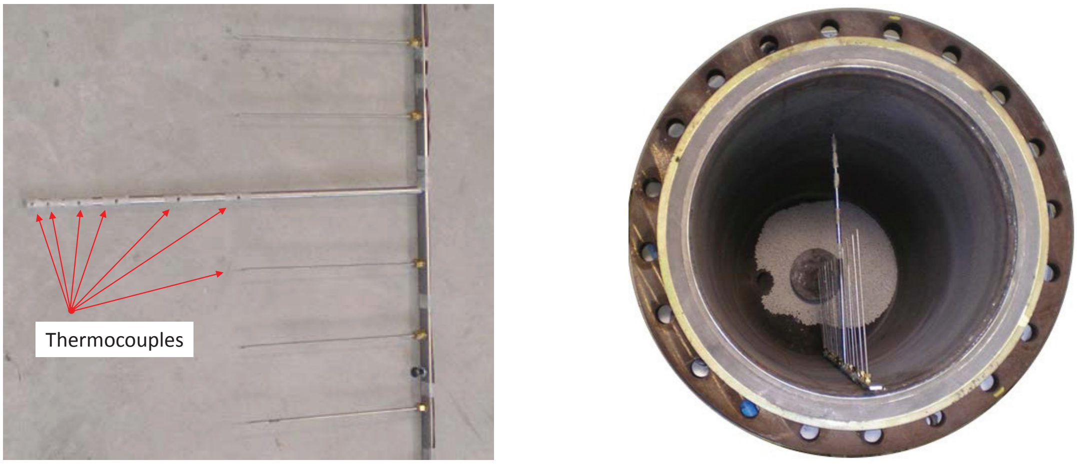

a) b)

Fig. 2. (a) thermocouple rack; (b) thermocouple rack installed in the tank

Before starting the charging phase, the initial temperature of the bed had to be stabilized. For this purpose the air initially flowed directly from the compressor to the tank, from bottom to top, through valves V1 and V2, then it was discharged into the atmosphere through valve V3. After this first step, the piping connecting the heater to the accumulator had to be heated until a stationary state was reached. In this second step valve V1 connected the compressor to the heater, thus allowing an increase in air temperature to the desired value, while the air was sent to the vent through V3. When the temperature detected by thermocouple TC (Figure 1a) reached the desired value, valve V3 was actuated to start the charging phase. The air moving along the porous bed from the top to the bottom heated the solid material and finally was vented through V2. During the discharging phase the valves were set as in the preliminary phase, and the cold air carried away the thermal energy stored in the accumulator.

This experimental set-up is suitable for investigating and evaluating performance of the storage system under different operating conditions by varying the mass flow rate, the aspect ratio, the particle dimension and the temperature range during the charging and discharging phases.

3. Mathematical model

Numerical simulations were carried out with a mathematical model developed in the Matlab-Simulink environment. A detailed description of this model is reported in a previous work [18]. It is a one-dimensional transient model where two energy equations (LTNE) are used to compute fluid and solid temperatures. It allows prediction of the porous bed thermal behavior along the main axis of symmetry by considering a uniform radial temperature distribution. The filler bed was assumed to be isotropic and homogeneous. The conduction among solid particles was neglected because the filler material was assumed to be spherical with a very small contact surface. Moreover, the Biot number of the particles is small enough to assume a uniform temperature distribution inside the beads. Airflow thermal properties are temperature-dependent, since they change considerably when operating in the temperature range of the tests. Natural convection and radiation are assumed negligible owing to sufficiently high flow velocity and moderate temperature values.

With these assumptions, the transient, one-dimensional, energy equations for fluid (1) and solid (2) phases along the axis of the bed are established as follows:

$$\varepsilon(\rho c_v)_f \frac{\partial T_f}{\partial t} + (\rho c_p)_f u_D \frac{\partial T_f}{\partial x} = k_{eff} \frac{\partial^2 T_f}{\partial x^2} + h_{sf}\alpha_{sf}(T_s - T_f) \tag{1}$$

$$(1-\varepsilon)(\rho c)_s \frac{\partial T_s}{\partial t} = h_{sf}\alpha_{sf}(T_f - T_s) \tag{2}$$

The specific surface area α_{sf} of the packed bed can be expressed, as suggested by Dullien [19], by the equation:

$$\alpha_{sf} = \frac{6(1-\varepsilon)}{d_p} \tag{3}$$

As it is known, the heat transfer coefficient between solid and fluid in the packed bed depends on the Nusselt number according to the equation:

$$h_{sf} = \frac{Nu k_f}{d_p} \tag{4}$$

Many literature correlations for the solid-to-fluid heat transfer coefficient in a packed bed were analyzed and compared. The most appropriate for this case study was a correlation based on a number of experimental findings, suitable for Re_p up to 8500, developed by Wakao [20]:

$$Nu = 2.0 + 1.1 \mathrm{Pr}^{1/3} \mathrm{Re}_p^{0.6} \tag{5}$$

where the Reynolds number is defined as follows:

$$\mathrm{Re}_p = \frac{\rho_f u_D d_p}{\mu_f} \tag{6}$$

4. Results

In the present work, a comparison of the predicted and measured temperature profile is presented. The comparison is based on a single cycle of charge-discharge of the storage material, implemented according to the procedure previously described. During the preliminary phase, a constant mass flow rate of 0.2 kg/s ±2.5% was sent into the reservoir, up to achieving an almost constant temperature T_{min} of about 38°C. The charging phase started when the thermocouple TC (Figure 1a) reached a stable value of 238 °C. Due to thermal losses and contact with the cold reservoir wall, the maximum temperature T_{max} at the top of the bed was always lower than the inlet temperature by about 10°C.

Figure 3a shows the behaviour of the experimental temperature profile along the bed in function of time during the charging phase, expressed in terms of the dimensionless temperature θ defined as:

$$\theta = \frac{T - T_{\min}}{T_{\max} - T_{\min}} \tag{7}$$

As can be seen in the figure 3a, the temperature profile in the upper part of the accumulator approached the maximum value in about half the time of full charge. The charging phase was considered complete when θ was equal to 0.1 in the outlet section of the porous bed (bottom), so that at the end of the charge the temperature decreased along the axis from the maximum value (θ=1) at the top of the bed to the minimum one (θ=0.1) at the bottom.

Figure 3b shows the evolution in time of the experimental temperature profiles along the bed axis during the charging phase, determined on the basis of the results in Figure 3a, together with the numerical ones determined according to different hypotheses. Temperature profiles are reported every fifth of the overall charging time. In Figure 3b, dotted lines refer to the numerical prediction under the hypothesis of constant temperature at the top of the bed (step-variation of temperature) and constant properties of storage material. Under these conditions, Figure 3b shows that numerical results are quite different from experimental ones, resulting in a higher temperature gradient with some agreement with experimental results only in the low temperature region. On the contrary, high disagreements can be observed in the high temperature region where the temperature profile is forced to the maximum temperature (θ=1) by the boundary condition assumed.

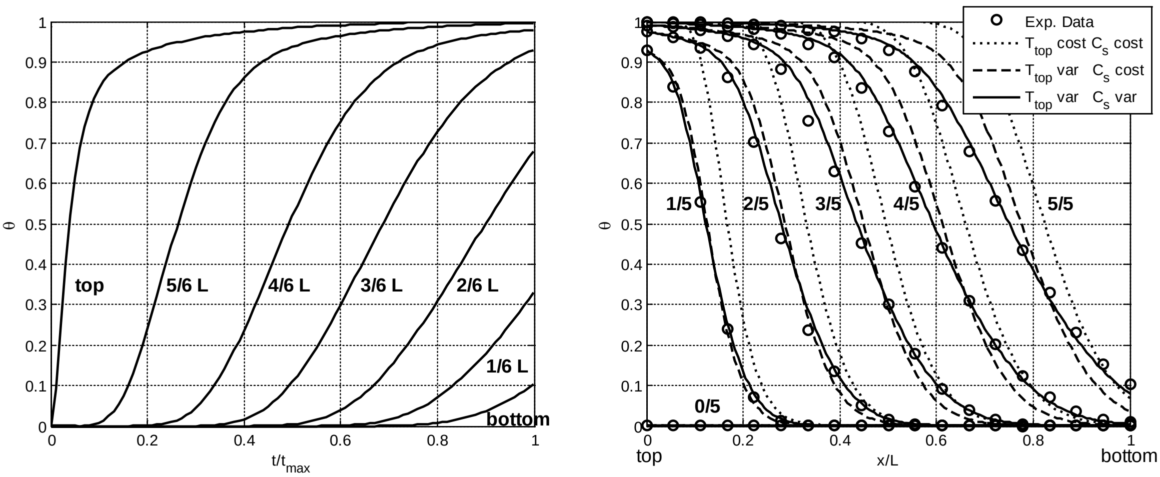

a) b)

Fig. 3. (a) temperature along the bed during the charging phase; (b) temperature profile during the charging phase.

On the other hand, step-variation in temperature at the top of the bed is not realistic and a better numerical simulation can be obtained on considering as input for the mathematical model a real temperature profile in the upper part of the accumulator as the experimental one in Figure 3a. This improved approach, represented by the dashed lines in Figure 3b, allows a better matching between numerical and experimental results, although differences still remain due to a different temperature gradient. A further improvement can be obtained by considering the thermal properties of the solid material as temperature-dependent [21]. The final numerical prediction, represented by the continuous lines, show a very good agreement with the experimental results. In the numerical prediction, the final temperature profile during the charging process becomes the initial profile for the discharging phase, where the air flow crosses the porous bed in the opposite direction with the same mass flow.

The discharging phase (Figure 4a) was considered completed when θ was equal to 0.9 in the outlet section of the porous bed (top). Owing to the slightly different starting temperature profile with respect to the experimental one, Figure 4a shows slightly larger differences between experimental and predicted results with respect to the charging phase.

Another significant result of the experimental investigation is represented by the radial distribution of the temperature in the bed shown in Figure 4b. About 40% of the radial length is strongly influenced by the tank wall, therefore the influence of the wall during the charging phase cannot be neglected in a correct evaluation of the energy stored by the solid material.

Although the one-dimensional model predicts well the axial temperature distribution of the bed, a 2-D model that considers the radial variation of the temperature is necessary to properly evaluate the energy performance of the accumulator. This requires the mathematical model to take into account the influence of the wall and the thermal loss to the outside. For this purpose, more detailed numerical simulations, using a commercial CFD code, are now in progress and results will be the object of future publications.

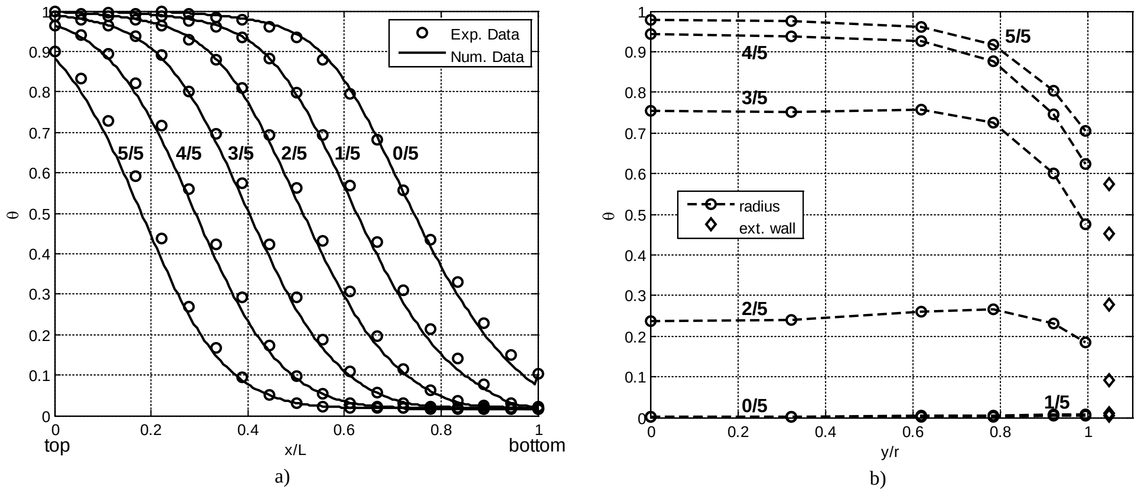

Fig. 4. (a) temperature profile during the discharging phase; (b) temperature along the radius during the charging phase

5. Conclusion

Because of the strategic importance of TES in solar power plants (as well as in adiabatic compressed air energy storage (CAES) systems and other energy conversion processes), in recent years several studies have been performed to investigate their characteristic performance. In this context, an ongoing research project at DIMCM focuses on TES based on solid material for storage using gas as HTF. The test-rig described here was designed to conduct extensive experimental investigations, with the aim of characterizing this kind of TES and verifying the reliability of the mathematical model previously developed. Experimental results presented in this work concern a cycle of partial charge and discharge of the TES system, but other tests have been conducted considering a wide range of operating conditions. In all cases the temperature measured along the axis of the reservoir showed the formation of the thermocline.

Moreover, in each test the experimental results showed a remarkable wall influence during the charging phase of the accumulator. This important finding confirms that to obtain a correct prediction of the energy stored and released during charge and discharge, at least a 2-D mathematical model must be implemented to take into account the radial variation of temperature in the bed. Nevertheless, the one-dimensional model presented in this work showed good agreement between numerical and experimental results when considering suitable boundary conditions at the top of the bed during the charging phase and temperature-dependent thermal properties of the heat transfer fluid and of the solid material.

Further results obtained from CFD simulations and more detailed experimental investigations will be the object of future publications.

Acknowledgements

This work was supported in the framework of the research project "Modelling control and testing of innovative thermal energy storage system" founded by the Regional Government of Sardinia, L.R. 7/2007 "Promotion of scientific research and technology innovation in Sardinia", project n° CRP-60193/2012.

References

[1] Laing D, Steinmann WD, Viebahn P, Gräter F, & Bahl C, Economic Analysis and Life Cycle Assessment of Concrete Thermal Energy Storage for Parabolic Trough Power Plants, Journal of Solar Energy Engineering, 132, 041013 ,2010.

[2] Trieb, Schillings, O'Sullivan, Pregger, Hoyer-Klick, Global Potential of Concentrating Solar Power. German Aerospace Center, Institute of Technical Thermodynamics: DLR: SolarPaces Conference Berlin, 2009.

[3] Medrano M, Gil A, Martorell I, Potau X, Cabeza L.F. State of the art on high temperature thermal energy storage for power generation. Part 2–Case Studies. Renewable & Sustainable Energy Reviews 2010;14:56–72

[4] Pilkington Solar International, GmbH. Survey of thermal storage for parabolic trough power plants. National Renewable Energy Laboratory; 2000 [SR-550-27925].

[5] Gil, A, Medrano M, and Cabeza LF, State of the art of high temperature storage in thermosolar plants L. F. University of Lleida, GREA Innovació Concurrent, Pere de Cabrera s/n 25001 Lleida, Spain, 2008.

[6] Yang Z, Suresh, Garimella V, Cyclic operation of molten-salt thermal energy storage in thermoclines for solar power plants, Applied Energy 103 (2013) 256–265.

[7] Gil, Medrano, Martorell, Lazaro, Dolado, Zalba, Cabeza, State of the art on high temperature for power generation. Part 1–Concepts, materials and modellization. Renewable & Sustainable Energy Reviews 2010;14:31–55.

[8] Gabbrielli R, Zamparelli C, Optimal design of a molten salt thermal storage tank for parabolic trough solar power plants, J. Sol. Energy Eng., 2009; 131, 041001 1-10;

[9] Cot-Gores J, Castell A, Cabeza LF, Thermochemical energy storage and conversion: A-state-of-the-art review of the experimental research under practical conditions; Renewable and Sustainable Energy Reviews 2012; 5207–5224.

[10] Van Lew J, Li P, Lik C, Karaki W, Stephens J, Analysis of Heat Storage and Delivery of a Thermocline Tank Having Solid Filler Material, Journal of Solar Energy Engineering, 2010.

[11] Kawanami T,Sakurai K Trans. of Japan Soc. of Mech. Eng. B **73** 2323; 2007.

[12] Wakao N & Kaguei S. Funazari T. Effect of fluid dispersion coefficients on particle-to-fluid heat transfer coefficients in packed beds. Chem Eng Sci; 1979; 35:325-36;

[13] Gnielinski, V, Fluid-particle heat transfer in flow through packed beds of solids. In: Stephan, P. (Ed.), VDI Heat Atlas. , Springer, Heidelberg, 2010 pp. 743–744.

[14] Tesfay, M & Venkatesan, M, Simulation of thermocline thermal energy storage system using C. International Journal of Innovation and Applied Studies, 2013; 3(2), pp.354–364.

[15] Schumann, T.E.W, Heat transfer: A liquid flowing through a porous prism. Journal of the Franklin Institute, 2010; 208(3), pp.405–416.

[16] Yang J, Wang Q, Zeng M, Nakayama A: Computational study of forced convective heat transfer in structured packed beds with spherical or ellipsoidal particles. Chemical Engineering Science 65, 2010, 726–738

[17] Flueckiger, SM, Yang Z. & Garimella SV, Thermomechanical Simulation of the Solar One Thermocline Storage Tank. Journal of Solar Energy Engineering, 2013; 134(4), p.041014.

[18] Cascetta M., Cau G., Puddu P., Serra F. Numerical investigation of a packed bed thermal energy storage system with different heat transfer fluids; Energy Procedia 45, 2014; 598 – 607.

[19] Dullien FAL. Porous media fluid transport and pore structure. New York. Academic Press. 1979.

[20] Wakao N & Kaguei S Heat and mass transfer in packed beds. New York Gordon and Breach Science Publishers Inc 1982.

[21] Anderson R. Samira Shiri, Hitesh Bindra, Morris J.F., Experimental results and modeling of energy storage and recovery in a packed bed of alumina particles, Applied Energy 2014, 119 p.521–529